THE JOURNAL OF PHYSICAL CHEMISTRY C

Article

pubs.acs.org/JPCC

Inter-Carbon Nanotube Contact and Thermal Resistances in Heat Transport of Three-Phase Composites

Feng Gong,[†] Hai M. Duong,*[,†] and Dimitrios V. Papavassiliou[‡]

[†]Department of Mechanical Engineering, National University of Singapore, Singapore, 117576 Singapore

[‡]School of Chemical, Biological, and Materials Engineering, University of Oklahoma, Norman, Oklahoma 73019, United States

ABSTRACT: Single-walled carbon nanotubes (SWNTs) tend to aggregate into bundles due to van der Waals forces during the fabrication of the composite. A computational model using an off-lattice Monte Carlo method is developed to systematically investigate the effects of SWNT bundles, the number of SWNTs per bundle and the thermal boundary resistance (TBR) at the SWNT−SWNT interfaces on the effective thermal conductivity (K_{eff}) of three-phase composites. It is found that the aggregation of the SWNTs in bundles can reduce significantly the K_{eff} of the composites with SWNTs oriented parallel or randomly to the heat flux direction, but it enhances slightly the K_{eff} of those with SWNTs perpendicular to the heat flux direction. The K_{eff} of the composites also decreases when more individual SWNTs aggregate in each bundle and with larger SWNT−SWNT TBR values. The thermal transport mechanism within the composites is dominated by a critical SWNT−SWNT TBR of 0.155×10^{-8} m^2K/W.

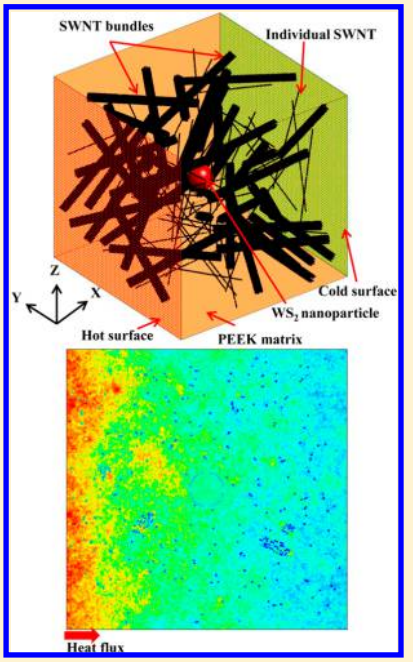

1. INTRODUCTION

Carbon nanotubes (CNTs) have been used as fillers to improve advanced multifunctional properties of polymer composites.[1] Due to intrinsic van der Waals forces, CNTs dispersed in a polymer matrix tend to aggregate into bundles. For heat transfer applications, the bundles limit the heat conduction for CNT-polymer composites.[2] Moreover, the thermal conductivity of an aggregated CNT bundle is usually lower than that of an individual CNT within the bundle due to the thermal boundary resistance (TBR) between adjacent CNTs.[3] This TBR may be incurred by the gaps between the adjacent CNTs and the weak van der Waals interaction,[4] much weaker than the strong sp^2 interaction between carbon atoms in the CNTs for phonon transport.[5] Therefore, polymer composites with dispersed CNT bundles inherit lower thermal conductivity than expected.[6]

In order to achieve uniform dispersion of the CNTs and avoid inter-CNT contact points in polymer composites, cost-ineffective treatments, such as covalent or noncovalent functionalization of CNTs,[7] and long-time sonication,[8] are commonly employed. It has been recently reported that a mixture of solid lubricant nanoparticles added with CNTs into a polymer matrix can improve the homogeneous distribution of CNTs.[9] In addition to the enhanced homogeneity of the CNT dispersions, the obtained three-phase composites can combine the properties and advantages of all components (i.e., CNTs, lubricant nanoparticles, and polymer matrix). Other novel three-phase composites have also been fabricated and studied for their multifunctional properties, such as CNT/graphene/polymer composites,[10] CNT/nanoparticle/polymer composites,[11] CNT/fiber/polymer composites,[12] and CNT-stabilized polymer blends.[13] Compared to two-phase composites, three-phase or multiphase composites can integrate the merits of all fillers and polymer into a hybrid system, resulting in more advanced properties of the composite materials. In these three-phase composites, the effective thermal properties may be influenced by the thermal properties and morphologies of both fillers, as well as their interactions. However, there are few comprehensive studies on the effect of the fillers and their interactions on the effective thermal conductivity of three-phase composites.

Received: January 22, 2015
Revised: March 6, 2015

DOI: 10.1021/acs.jpcc.5b00651
J. Phys. Chem. C XXXX, XXX, XXX−XXX

Effective medium theory (EMT) and its modifications can be applied to predict the effective thermal conductivity (K_{eff}) of CNT-dispersed polymer composites.[14] While such predictions take into account the diameter and length of CNTs, they assume a perfect dispersion of single CNTs and ignore the CNT bundles and the effect of CNT orientation. However, in three-phase composites, scanning electron microscopy (SEM) images show that CNT bundles, individual CNTs, and lubricant nanoparticles coexist in the polymer matrix.[9] Common EMT-based calculations[14] cannot predict accurately the K_{eff} of complex CNT-polymer composites where individual CNTs and CNT bundles coexist. The inter-CNT contact within the CNT bundles may cause smaller K_{eff} for the composites than when the TBR is only between CNTs and the polymer matrix.[15] The CNT-CNT TBRs may dominate heat transfer and limit heat conduction in the complex CNT-polymer composites.[2,16]

The random walker model developed by Duong et al.[15,17] can take into account the CNT bundle configuration and can be used to explore the effect of CNT-CNT TBR in two-phase composites. But prior studies did not investigate the composites with CNT bundles having random orientations and complex morphology (e.g., different number of CNTs in a bundle). Moreover, their model may fail to represent accurately the three-phase composites when considering the interaction between the fillers. In order to overcome the limitations of the previous models,[14,15,17,18] appropriate simulation approaches are desired to predict more accurately the K_{eff} of composites with complex morphology, CNT local agglomeration, CNT bundles, and TBRs at all interfaces.

We have developed an advanced mesoscopic model using an off-lattice Monte Carlo method to study the thermal transport phenomena and limitations in three-phase poly(ether ether ketone) (PEEK) composites having single-walled carbon nanotubes (SWNTs) and tungsten disulfide (WS_2) nanoparticles.[19] Our model predicted more accurately the K_{eff} of three-phase composites than previous models, such as EMTs, by taking into account: (i) various aspect ratios and orientations of the SWNTs, (ii) synergistic effects of the SWNTs and WS_2 nanoparticles, and (iii) the TBRs between the nanofillers (SWNTs and WS_2) and the PEEK matrix. But our previous model ignored the effects of SWNT bundles and SWNT inter-contact,[19] which cannot be avoided in the composite fabrication procedures.[9] To replicate practical three-phase composites and predict more accurately their K_{eff}, in this work we eliminate the assumptions of the previous three-phase model[19] and investigate comprehensively the effects of the number of SWNT bundles, the SWNT number per bundle, and the SWNT−SWNT TBRs on the K_{eff} of the three-phase composites. The simulation results of our present work and our previous works[19,20] can provide quantitative perspectives about the thermal transport mechanisms and limitations of complex multiphase systems, including two- and three-phase polymer composites, metal composites, nanofluids, and biological systems having CNTs.[21] The developed model promises to bridge the atomistic approaches (e.g., molecular dynamic simulations)[22] and the continuum approaches (e.g., rule of mixture and Halpin−Tsai models)[2,23] by taking into account the interfacial thermal resistances and the complex configurations of composites (e.g., random-oriented SWNTs, SWNT bundles, larger aspect ratio, and number of SWNTs).

2. SIMULATION METHODOLOGY

More details of the algorithm development can be found in our previous works.[20,21] In brief, thermal energy is quantified through a large quantity of discrete thermal walkers having the same energy.[24] The transfer of heat is considered as the result of the Brownian motion of the thermal walkers in the polymer matrix, which is described by the random motion of the thermal walkers in each space direction.[25] The random movement occurs in jumps that take values from a normal distribution with a zero mean and a standard deviation σ, expressed as[26]

$$\sigma = \sqrt{2D_m \Delta t} \quad (1)$$

where D_m is the PEEK thermal diffusivity and Δt is the time increment of the simulation.[26] When a walker jumps to the SWNT−PEEK interface, it may jump into the SWNT with a probability $f_{m\text{-}CNT}$ or remain within the PEEK matrix with a probability $(1 - f_{m\text{-}CNT})$. The probability is a function of the TBR between PEEK and SWNT, $R_{m\text{-}CNT}$, obtained using the acoustic mismatch theory (AMT):[27]

$$f_{m-CNT} = 4/(\rho C_p \nu R_{m\text{-}CNT}) \quad (2)$$

where ρ is the PEEK density, C_p is the PEEK specific heat, and ν is the sound velocity in PEEK. Due to the ballistic phonon transport and ultrahigh thermal conductivity in the SWNT,[28] thermal walkers are assumed to travel at an infinite speed inside the SWNT.[29] The walker is allowed to exit from a SWNT to the matrix by using another probability $f_{CNT\text{-}m}$, which is related to $f_{m\text{-}CNT}$ in a way that satisfies the second thermodynamic theorem:[24,30]

Table 1. Material Properties and Simulation Parameters

basic properties			
	PEEK	WS_2	SWNT
density (kg/m^3)	1320	7400	2100
specific heat capacity [J/(kg K)]	1136	330	841
thermal conductivity [W/(m K)]	0.23	1.675	∼3500
speed of sound (m/s)	2300	4000	8000
geometry			
computational domain size (nm^3)	925 × 925 × 925		
WS_2 sphere nanoparticle diameter (nm)	110		
SWNT diameter (nm)	2		
SWNT length (nm)	500		
WS_2 mass fraction (%)	0.5		
SWNT mass fraction (%)	0.3		
number of SWCNT	960		
interfacial thermal properties			
TBR at the SWNT−PEEK interface, $R_{m-CNT} \times 10^{-8}$ m^{2}K/W (f_{m-CNT})	1.158 (0.1)		
TBR at the WS_2−PEEK interface, $R_{m-WS2} \times 10^{-8}$ m^{2}K/W (f_{m-WS2})	0.0116 (1.0)		
TBR at the SWNT−SWNT interface, $R_{CNT-CNT} \times 10^{-8}$ m^{2}K/W	0.0615, 0.205, 0.615, 2.05, 6.15		
phonon transmission probability at the SWNT−SWNT interface, $f_{CNT-CNT}$	1.0, 0.3, 0.1, 0.03, 0.01		
thermal equilibrium factors C_f	$C_{f-WS2} = 0.285$, $C_{f-CNT} = 0.35$		
simulation parameters			
number of computational cells	300 × 300 × 300		
number of thermal walkers	40000		
time increment (ps)	3		
number of time steps	1000000		

DOI: 10.1021/acs.jpcc.5b00651
J. Phys. Chem. C XXXX, XXX, XXX−XXX

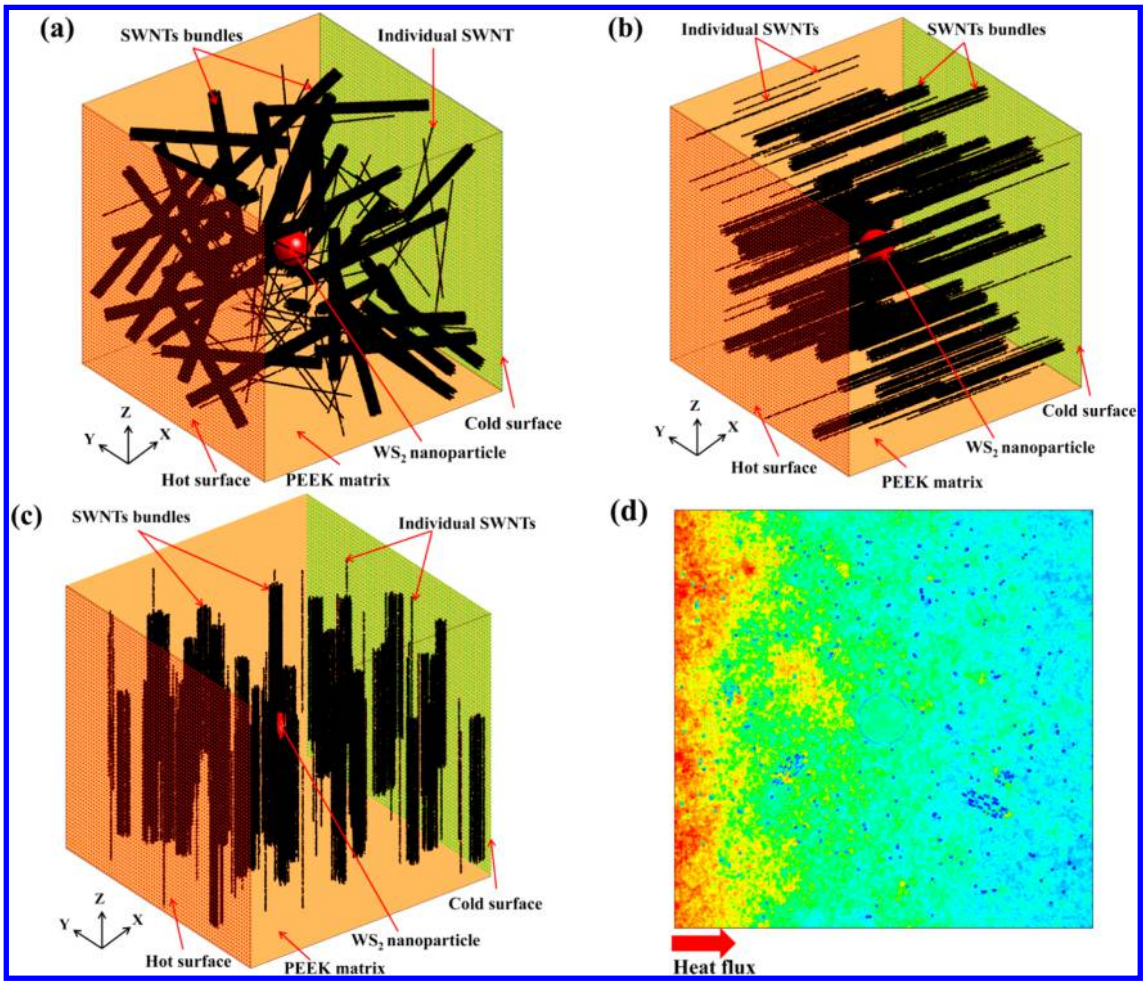

Figure 1. Schematic plot of the computational model: (a) a 110 nm diameter WS_2 nanoparticle is located in the center of a PEEK cube (925 × 925 × 925 nm). 960 SWNTs (2 nm in diameter and 500 nm in length) forms 45 bundles having 20 SWNTs in each bundle and 60 unbundled SWNTs. The uniform red and green dot planes are the hot and cooled surfaces, respectively. (b) Composite with individual SWNTs and SWNT bundles oriented parallel to the heat flux direction. (c) Composite with individual SWNTs and SWNT bundles oriented perpendicularly to the heat flux direction. (d) A contour plot of thermal walkers along the heat flux in the center $x-y$ plane (z = 150 grid) of the three-phase composite at the 1000000 time step.

$$V_{\mathrm{CNT}} f_{\mathrm{CNT-m}} = C_{f-\mathrm{CNT}} \sigma_{\mathrm{m}} A_{\mathrm{CNT}} f_{\mathrm{m-CNT}} \tag{3}$$

wherein V_{CNT} and A_{CNT} are the volume and surface area of a SWNT and σ_{m} is the standard deviation of Brownian motion in the PEEK matrix. $C_{f-\mathrm{CNT}}$ is a coefficient that can be called the thermal equilibrium factor at the PEEK−SWNT interface, which is dependent on the geometry of the SWNTs and the interfacial area between the SWNT and the matrix.

Similar to the motion within the PEEK matrix, the thermal walkers inside a WS_2 nanoparticle also jump randomly in three directions but with a different thermal diffusivity (that of the WS_2). The governing probability for the thermal walker entering the WS_2 nanoparticles, $f_{\mathrm{m-WS2}}$, is also determined by the AMT as expressed in eq 2. At the WS_2−PEEK interface, thermal walkers from either the WS_2 side or the PEEK side behave similarly to the walkers crossing the PEEK-SWNT interface from the PEEK matrix. However, due to the different motion of walkers inside WS_2 nanoparticles and inside the SWNTs, the relation between the two probabilities governing the thermal walkers' movements crossing the WS_2−PEEK interface, $f_{\mathrm{m\text{-}WS_2}}$ and $f_{\mathrm{WS_2\text{-}m}}$, is different from eq 3, and is as follows:[19]

$$f_{\mathrm{WS_2\text{-}m}} = C_{f\text{-}\mathrm{WS_2}} \frac{(r+\sigma_{\mathrm{m}})^3 - r^3}{r^3 - (r-\sigma_{\mathrm{WS_2}})^3} f_{\mathrm{m\text{-}WS_2}} \tag{4}$$

where $\sigma_{\mathrm{WS_2}}$ is the standard deviation of the Brownian motion inside the WS_2 nanoparticle. r is the radius of WS_2 nanoparticles, and $C_{f\text{-}\mathrm{WS_2}}$ is the thermal equilibrium factor at the WS_2−PEEK interface. All the parameters used in the simulations can be found in Table 1.

The assumptions of the model described in this paper are[31] (1) collisions between thermal walkers are not considered: walker−walker collisions reflect the phonon−phonon scattering in the composites, which is much weaker than the phonon scattering by the disordered matrix materials. We ignore this nonlinear collision between thermal walkers in the current work. (2) Thermal properties of all components do not change with temperature over the modeled range. (3) TBRs are identical at the same interface for thermal walkers entering or exiting from a component. (4) WS_2 nanoparticles are assumed to disperse well without aggregating into clusters due to their lubrication properties. (5) The bulk properties of the polymer are used in the current model, while the crystallinity of the polymer is not taken into account. (6) Walkers bounce back

DOI: 10.1021/acs.jpcc.5b00651
J. Phys. Chem. C XXXX, XXX, XXX−XXX

when jumping outside the computational box in the x direction. This boundary condition is used to avoid walkers entering and immediately leaving, thus to fix the constant heat flux in the x direction. Periodic boundary conditions are applied in the y- and z-directions to achieve the energy conservation. And (7) Computational domain has the same initial temperature.

The individual SWNTs are parallel to each other to form SWNT bundles, and then the SWNT bundles and the unbundled individual SWNTs are randomly distributed in the PEEK matrix as shown in Figure 1a. Both the bundled SWNTs and the individual SWNTs have the same length (500 nm) and diameter (2 nm).[9a] When a thermal walker travels inside a SWNT bundle, it may jump among the bundled SWNTs depending on the TBR at the SWNT−SWNT contact, $R_{CNT-CNT}$. The $R_{CNT-CNT}$ is quantified by a probability of the thermal walkers jumping among the bundled SWNTs, $f_{CNT-CNT}$, obtained using the acoustic mismatch theory.[32] A constant heat flux is applied to determine the K_{eff} of the SWNT/WS_2/PEEK composites by releasing 40000 hot walkers from one side of the computational box (i.e., a hot side at x = 0) and another 40000 cold walkers (carrying negative energy) from the opposite side, as seen in Figure 1. When reaching steady state, the temperature at every position of the computational box can be determined by using a 300 × 300 × 300 grid mesh in the computational box and counting the number of hot and cold walkers in each grid cell.[20] The K_{eff} of the SWNT/WS_2/PEEK composites can be determined by the ratio of the temperature gradients along the heat flux in the composite and the pure matrix without fillers, as expressed as

$$q'' = -K_{eff}\frac{dT_c}{dx} = -K_m\frac{dT_m}{dx} \quad (5)$$

where T_c and T_m are the temperatures along the heat flux direction in the composites and in the neat PEEK model, respectively. q'' is the heat flux and K_m is the thermal conductivity of PEEK (0.23 W/m K). So the K_{eff} can be obtained as

$$K_{eff} = K_m\frac{dT_m}{dx}/\frac{dT_c}{dx} \quad (6)$$

This paper focuses on the effects of the inter-SWNT contact, various SWNT orientations, the number of SWNT bundles, and the individual SWNT number per bundle on the K_{eff} of SWNT/WS_2/PEEK composites. The developed model can be applied to double-walled CNTs, multiwalled CNTs, and even graphene nanosheets.[15,33] The effects of TBRs between the nanofillers (SWNT and WS_2) and the PEEK matrix, nanofiller weight fractions, and the individual SWNT morphologies can be found in our previous work.[19] A 0.3/0.5/99.2 SWNT/WS_2/PEEK composite, in which weight fractions of the SWNTs, the WS_2 nanoparticles, and the PEEK matrix are 0.3%, 0.5%, and 99.2%, respectively, is chosen as the study case.[9a] At this mass fraction of SWNTs (0.3 wt %), 960 SWNTs are involved to construct the composite.[19]

3. RESULTS AND DISCUSSIONS

3.1. Effects of the Number of SWNT Bundles on the K_{eff} of the Three-Phase Composites. We present in Figure 2, the effect of the number of SWNT bundles (0−48) on the K_{eff} of the SWNT/WS_2/PEEK composites having different SWNT bundle orientations (parallel, perpendicular, and random to the heat flux direction), as shown in Figure 1.

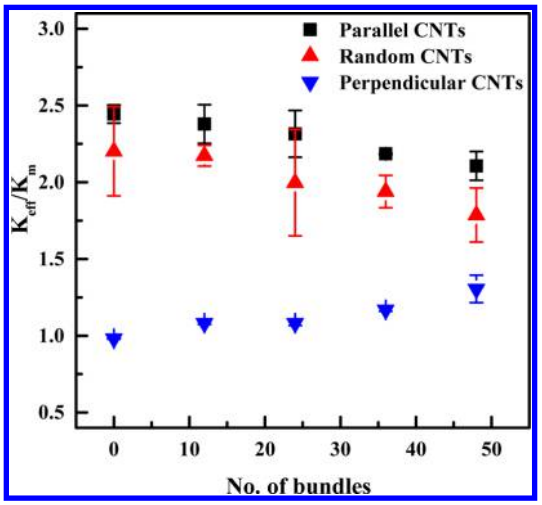

Figure 2. Effects of the number and orientation of the SWNT bundles on the K_{eff} of the SWNT/WS_2/PEEK composites. The TBRs of SWNT-PEEK (1.158×10^{-8} m^2K/W), WS_2−PEEK (0.0116×10^{-8} m^2K/W), and SWNT−SWNT (0.615×10^{-8} m^2K/W) are kept constant. Each data point is averaged from 3 different simulations with the different initial distributions of the individual SWNTs and the SWNT bundles.

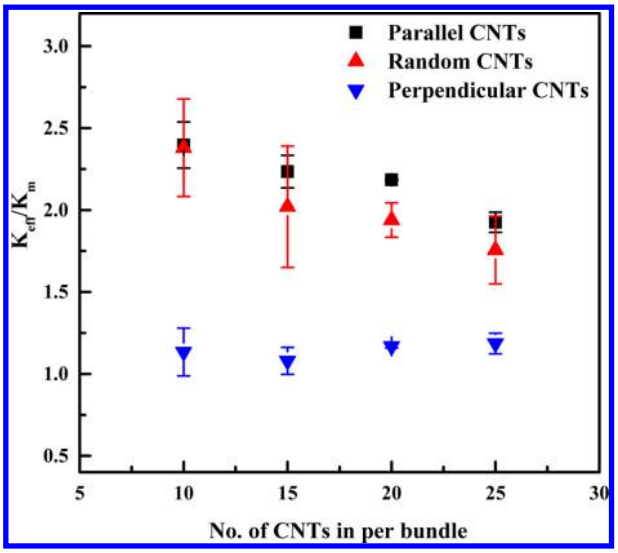

Figure 3. Effect of the number of individual SWNTs per bundle on the K_{eff} of the SWNT/WS_2/PEEK composites having different SWNT orientations. A total of 960 SWNTs and 36 bundles are kept constant.

While the number of SWNTs is kept at 960 and each bundle has 20 individual SWNTs, the extent by which SWNTs are in contact with each other varies from no SWNTs in contact (0 bundles) to all SWNTs in contact (48 bundles). Compared to the pure PEEK matrix, the K_{eff} of the composites having 48 SWNT bundles oriented parallel or randomly to the heat flux can be enhanced by ~2.3 or ~1.7 times, respectively. The K_{eff} decreases with increasing the number of SWNT bundles because (i) more SWNT bundles cause more local SWNT agglomeration and reduce the uniform distribution of the individual SWNTs in the PEEK matrix;[34] and (ii) the SWNT−SWNT TBRs within the bundles inhibit heat transfer along the heat flux direction. When the SWNT bundles are perpendicular to the heat flux, K_{eff} slightly increase, approximately by 40% when the number of SWNT bundles increases to 48. This

DOI: 10.1021/acs.jpcc.5b00651
J. Phys. Chem. C XXXX, XXX, XXX−XXX

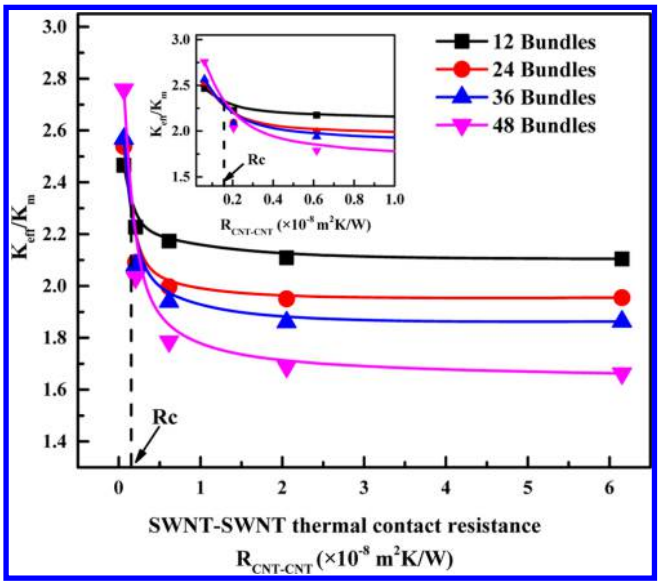

Figure 4. Effect of the SWNT−SWNT TBR on the K_{eff} of the SWNT/WS_2/PEEK composites having 12−48 SWNT bundles. The individual SWNT number in each bundle is kept at 20. The TBRs between nanofillers (SWNT and WS_2) and PEEK matrix are kept constant as Figure 3. The critical TBR (dash line) is estimated to be $R_c = 0.155 \times 10^{-8}$ m^2K/W by intersecting the K_{eff} curves of different SWNT bundles.

happens as the bundles formed from 20 individual SWNTs have bigger diameter and can allow the heat to transfer more easily in the direction of their radius.

3.2. Effects of the Number of Individual SWNTs Per Bundle on the K_{eff} of the Three-Phase Composites. The effect of the number of individual SWNTs in each bundle on the K_{eff} of the composites is presented in Figure 3. While a total of 960 SWNTs and 36 bundles are kept constant, the number of individual SWNTs in each bundle is varied from 10 to 25 with an interval of 5. For composites having the SWNTs oriented parallel or randomly to the heat flux direction, the K_{eff} decreases with increasing the number of individual SWNTs in each bundle. With the same number of bundles, more individual SWNTs aggregated in each bundle cause the distribution of the SWNTs in the composites to be nonuniform. A bundle with more aggregated SWNTs has a larger diameter and a lower aspect ratio (length/diameter), which may also decrease the K_{eff}.[35] The finding is consistent with previous works.[19,25] The phonon coupling between the SWNTs and the PEEK occurs only via low-frequency vibrations.[36] The lower aspect ratio may enhance the SWNT bundle stiffness and weaken the low-frequency vibrations in the SWNT bundles. This leads to a larger SWNT-PEEK TBR[5] and then a reduction of the composite K_{eff}.[37] The number of individual SWNTs in each bundle seems to have no significant effect on the K_{eff} when the SWNTs are perpendicular to the heat flux. This may be explained as follows: when SWNTs are oriented perpendicular to the heat flux, individual SWNTs cannot enhance the K_{eff} of the composites.[19] Since the addition of few CNTs does not much alter the bundle diameter, and only SWNT bundles may slightly improve the K_{eff} of the composites, when the number of SWNT bundles is fixed, the K_{eff} of the composites is also expected to remain nearly constant.

3.3. Effects of the SWNT−SWNT TBR on the K_{eff} of the Three-Phase Composites. In Figure 4, we present the effect of the SWNT−SWNT TBR on the K_{eff} of the three-phase composites. Results for composites with different degree of SWNT aggregation and with random dispersion in the composites are presented. Composites having randomly oriented SWNTs are chosen for further study as they replicate most of the practical SWNT-dispersed composites fabricated in the experiments. The SWNT−SWNT TBR in the bundles, $R_{CNT-CNT}$, was varied in the range from 0.0615×10^{-8} to 6.1530×10^{-8} m^2K/W.[15] The simulation results are summarized in Table 2. When the number of SWNT bundles is constant, the K_{eff} of the composites decreases as the $R_{CNT-CNT}$ increases.[15,17] A larger $R_{CNT-CNT}$ more significantly impedes the transfer of heat between bundled SWNTs, inducing a lower K_{eff} of the composites. Surprisingly, the heat

Table 2. Effects of the SWNT Bundle Number, the Individual SWNT Number Per Bundle, and the $R_{CNT-CNT}$ on the (K_{eff}/K_m) of the SWNT/WS_2/PEEK Composites*

	K_{eff}/K_m								
	$R_{CNT-CNT}$ (× 10^{-8} m^2K/W) ($f_{CNT-CNT}$)								
	0.0615 (1.0)			0.615 (0.1)			6.15 (0.01)		
	individual SWNT number in each bundle			individual SWNT number in each bundle			individual SWNT number in each bundle		
no. of bundles	15	20	25	15	20	25	15	20	25
Bundled and Unbundled SWNTs are Parallel to the Heat Flux									
12	2.380	2.375	2.328	2.368	2.379	2.248	2.408	2.366	2.279
24	2.487	2.341	2.093	2.426	2.315	2.101	2.386	2.239	2.157
36	2.241	2.217	1.914	2.234	2.185	1.921	2.240	2.139	1.955
Bundled and Unbundled SWNTs are Random to the Heat Flux									
12	2.395	2.258	2.237	2.119	2.173	1.972	2.106	2.104	1.921
24	2.399	2.308	2.292	2.143	1.997	1.940	2.067	1.955	1.886
36	2.619	2.568	2.311	2.021	1.939	1.756	1.921	1.863	1.677
Bundled and Unbundled SWNTs are Perpendicular to the Heat Flux									
12	1.062	1.176	1.044	1.040	1.082	1.022	0.990	1.007	0.990
24	1.136	1.183	1.170	1.062	1.082	1.091	1.008	0.998	1.008
36	1.128	1.319	1.358	1.081	1.168	1.186	1.008	1.031	1.021

*The result in each case is averaged from the results of three simulations with the different spatial distributions of the individual SWNTs and the SWNT bundles. TBRs of SWNT-PEEK (1.158×10^{-8} m^2K/W) and WS_2−PEEK (0.0116×10^{-8} m^2K/W) are kept constant in all the simulations.

DOI: 10.1021/acs.jpcc.5b00651
J. Phys. Chem. C XXXX, XXX, XXX−XXX

transfer mechanism is dominated by a critical SWNT−SWNT TBR, R_c, which is estimated to be 0.155×10^{-8} m^2K/W. This value is obtained based on the data shown in Figure 4, by choosing as the critical point the point at which the lines intersect (see the inset figure). When the $R_{CNT-CNT}$ is lower than the R_c, more bundles lead to significant increase of the K_{eff} of the composite. This can be explained physically, since at very low $R_{CNT-CNT}$, more contact between SWNTs may allow more heat transport between individual SWNTs in a bundle. However, when the $R_{CNT-CNT}$ is larger than the R_c, the K_{eff} of the composites with more bundles decreases dramatically because the individual SWNTs may dominate the heat transfer. A large SWNT−SWNT TBR in the bundles may arise from the weak van der Waals interactions for phonon coupling and the strong phonon−phonon scattering at interfaces.[3b,38] Covalent functionalization can be applied to shift the van der Waals interactions into the strong sp^2/sp^3 interactions for phonon coupling[39] and to weaken the phonon−phonon scattering at interfaces to reduce the SWNT−SWNT TBRs.[40]

4. CONCLUSIONS

In summary, the effects of SWNT bundle configurations on the K_{eff} of the SWNT/WS_2/PEEK composites having different SWNT orientations are investigated by the off-Lattice Monte Carlo method. Except for the cases of heat flux perpendicular to the SWNTs, the simulation results show that the more SWNT bundles and the more individual SWNTs in each bundle can reduce the K_{eff} of the SWNT/WS_2/PEEK composites. The same is true when the TBR at the SWNT−SWNT contact increases. A critical SWNT−SWNT TBR, which may dominate the heat transfer mechanism in the three-phase composites, is estimated to be $R_c = 0.155 \times 10^{-8}$ m^2K/W. We can speculate that the K_{eff} of the three-phase composites can be enhanced by proper covalent functionalization of the SWNTs. The functionalization of SWNTs can uniformly disperse SWNTs in the composites and reduce the TBRs at the SWNT−SWNT contact and at the SWNT−polymer interfaces.[41]

AUTHOR INFORMATION

Corresponding Author

*E-mail: mpedhm@nus.edu.sg.

Notes

The authors declare no competing financial interest.

ACKNOWLEDGMENTS

The authors would like to thank SERC 2011 PSF Funding R-265-000-424-305 and Temasek Laboratories @ NUS Funding R-394-001-077-232 for the financial support. This work was done while Dimitrios Papavassiliou was serving at the National Science Foundation (NSF). Any opinion, findings, and conclusions or recommendations expressed in this material are those of the authors and do not necessarily reflect the views of the NSF.

REFERENCES

(1) De Volder, M. F. L.; Tawfick, S. H.; Baughman, R. H.; Hart, A. J. Carbon Nanotubes: Present and Future Commercial Applications. *Science* **2013**, *339* (6119), 535−539.

(2) Han, Z. D.; Fina, A. Thermal Conductivity of Carbon Nanotubes and Their Polymer Nanocomposites: A Review. *Prog. Polym. Sci.* **2011**, *36* (7), 914−944.

(3) (a) Kim, P.; Shi, L.; Majumdar, A.; McEuen, P. L. Thermal Transport Measurements of Individual Multiwalled Nanotubes. *Phys. Rev. Lett.* **2001**, *87* (21), 215502. (b) Prasher, R. Thermal Boundary Resistance and Thermal Conductivity of Multiwalled Carbon Nanotubes. *Phys. Rev. B* **2008**, *77* (7), 075424. (c) Volkov, A. N.; Zhigilei, L. V. Scaling Laws and Mesoscopic Modeling of Thermal Conductivity in Carbon Nanotube Materials. *Phys. Rev. Lett.* **2010**, *104* (21), 215902.

(4) Hone, J.; Batlogg, B.; Benes, Z.; Johnson, A. T.; Fischer, J. E. Quantized Phonon Spectrum of Single-Wall Carbon Nanotubes. *Science* **2000**, *289* (5485), 1730−1733.

(5) Zhong, H.; Lukes, J. R. Interfacial Thermal Resistance between Carbon Nanotubes: Molecular Dynamics Simulations and Analytical Thermal Modeling. *Phys. Rev. B* **2006**, *74* (12), 125403.

(6) Choi, E. S.; Brooks, J. S.; Eaton, D. L.; Al-Haik, M. S.; Hussaini, M. Y.; Garmestani, H.; Li, D.; Dahmen, K. Enhancement of Thermal and Electrical Properties of Carbon Nanotube Polymer Composites by Magnetic Field Processing. *J. Appl. Phys.* **2003**, *94* (9), 6034−6039.

(7) Dyke, C. A.; Tour, J. M. Covalent Functionalization of Single-Walled Carbon Nanotubes for Materials Applications. *J. Phys. Chem. A* **2004**, *108* (51), 11151−11159.

(8) Tchoul, M. N.; Ford, W. T.; Ha, M. L. P.; Chavez-Sumarriva, I.; Grady, B. P.; Lolli, G.; Resasco, D. E.; Arepalli, S. Composites of Single-Walled Carbon Nanotubes and Polystyrene: Preparation and Electrical Conductivity. *Chem. Mater.* **2008**, *20* (9), 3120−3126.

(9) (a) Naffakh, M.; Diez-Pascual, A. M.; Gomez-Fatou, M. A. New Hybrid Nanocomposites Containing Carbon Nanotubes, Inorganic Fullerene-Like WS2 Nanoparticles and Poly(ether ether ketone) (PEEK). *J. Mater. Chem.* **2011**, *21* (20), 7425−7433. (b) Naffakh, M.; Diez-Pascual, A. M.; Marco, C.; Ellis, G. Morphology and Thermal Properties of Novel Poly(Phenylene Sulfide) Hybrid Nanocomposites Based on Single-Walled Carbon Nanotubes and Inorganic Fullerene-Like WS2 Nanoparticles. *J. Mater. Chem.* **2012**, *22* (4), 1418−1425.

(10) (a) Yu, A. P.; Ramesh, P.; Sun, X. B.; Bekyarova, E.; Itkis, M. E.; Haddon, R. C. Enhanced Thermal Conductivity in a Hybrid Graphite Nanoplatelet: Carbon Nanotube Filler for Epoxy Composites. *Adv. Mater. (Weinheim, Ger.)* **2008**, *20* (24), 4740−4744. (b) Gupta, T. K.; Singh, B. P.; Mathur, R. B.; Dhakate, S. R. Multi-walled carbon nanotube−graphene−polyaniline multiphase nanocomposite with superior electromagnetic shielding effectiveness. *Nanoscale* **2014**, *6*, 842−851.

(11) Socher, R.; Krause, B.; Hermasch, S.; Wursche, R.; Pötschke, P. Electrical and Thermal Properties of Polyamide 12 Composites with Hybrid Fillers Systems of Multiwalled Carbon Nanotubes and Carbon Black. *Compos. Sci. Technol.* **2011**, *71* (8), 1053−1059.

(12) (a) Liao, W. H.; Tien, H. W.; Hsiao, S. T.; Li, S. M.; Wang, Y. S.; Huang, Y. L.; Yang, S. Y.; Ma, C. C. M.; Wut, Y. F. Effects of Multiwalled Carbon Nanotubes Functionalization on the Morphology and Mechanical and Thermal Properties of Carbon Fiber/Vinyl Ester Composites. *ACS Appl. Mater. Interfaces* **2013**, *5* (9), 3975−3982. (b) Diez-Pascual, A. M.; Ashrafi, B.; Naffakh, M.; Gonzalez-Dominguez, J. M.; Johnston, A.; Simard, B.; Martinez, M. T.; Gomez-Fatou, M. A. Influence of carbon nanotubes on the thermal, electrical and mechanical properties of poly(ether ether ketone)/glass fiber laminates. *Carbon* **2011**, *49* (8), 2817−2833.

(13) Cheng, H. K. F.; Basu, T.; Sahoo, N. G.; Li, L.; Chan, S. H. Current Advances in the Carbon Nanotube/Thermotropic Main-Chain Liquid Crystalline Polymer Nanocomposites and Their Blends. *Polymers* **2012**, *4* (2), 889−912.

(14) Nan, C. W.; Liu, G.; Lin, Y. H.; Li, M. Interface Effect on Thermal Conductivity of Carbon Nanotube Composites. *Appl. Phys. Lett.* **2004**, *85* (16), 3549−3551.

(15) Duong, H. M.; Yamamoto, N.; Bui, K.; Papavassiliou, D. V.; Maruyama, S.; Wardle, B. L. Morphology Effects on Nonisotropic Thermal Conduction of Aligned Single-Walled and Multi-Walled Carbon Nanotubes in Polymer Nanocomposites. *J. Phys. Chem. C* **2010**, *114* (19), 8851−8860.

(16) Marconnett, A. M.; Yamamoto, N.; Panzer, M. A.; Wardle, B. L.; Goodson, K. E. Thermal Conduction in Aligned Carbon Nanotube-Polymer Nanocomposites with High Packing Density. *ACS Nano* **2011**, *5* (6), 4818−4825.

DOI: 10.1021/acs.jpcc.5b00651
J. Phys. Chem. C XXXX, XXX, XXX−XXX

(17) Duong, H. M.; Yamamoto, N.; Papavassiliou, D. V.; Maruyama, S.; Wardle, B. L. Inter-Carbon Nanotube Contact in Thermal Transport of Controlled-Morphology Polymer Nanocomposites. *Nanotechnology* **2009**, *20* (15), 155702.
(18) Nan, C. W.; Shi, Z.; Lin, Y. A Simple Model for Thermal Conductivity of Carbon Nanotube-Based Composites. *Chem. Phys. Lett.* **2003**, *375* (5−6), 666−669.
(19) Gong, F.; Bui, K.; Papavassiliou, D. V.; Duong, H. M. Thermal Transport Phenomena and Limitations in Heterogeneous Polymer Composites Containing Carbon Nanotubes and Inorganic Nanoparticles. *Carbon* **2014**, *78* (0), 305−316.
(20) Gong, F.; Papavassiliou, D. V.; Duong, H. M. Off-Lattice Monte Carlo Simulation of Heat Transfer through Carbon Nanotube Multiphase Systems Taking into Account Thermal Boundary Resistances. *Numer. Heat Transfer, Part A* **2014**, *65* (11), 1023−1043.
(21) Gong, F.; Hongyan, Z.; Papavassiliou, D. V.; Bui, K.; Lim, C.; Duong, H. M. Mesoscopic Modeling of Cancer Photothermal Therapy Using Single-Walled Carbon Nanotubes and near Infrared Radiation: Insights through an Off-Lattice Monte Carlo Approach. *Nanotechnology* **2014**, *25* (20), 205101.
(22) Khare, K. S.; Khabaz, F.; Khare, R. Effect of Carbon Nanotube Functionalization on Mechanical and Thermal Properties of Cross-Linked Epoxy−Carbon Nanotube Nanocomposites: Role of Strengthening the Interfacial Interactions. *ACS Appl. Mater. Interfaces* **2014**, *6* (9), 6098−6110.
(23) Lin, W. Modeling of Thermal Conductivity of Polymer Nanocomposites. In *Modeling and Prediction of Polymer Nanocomposite Properties*; Wiley-VCH: Weinheim, Germany, 2013; pp 169−200.
(24) Duong, H. M.; Papavassiliou, D. V.; Mullen, K. J.; Wardle, B. L.; Maruyama, S. Calculated Thermal Properties of Single-Walled Carbon Nanotube Suspensions. *J. Phys. Chem. C* **2008**, *112* (50), 19860−19865.
(25) Duong, H. M.; Papavassiliou, D. V.; Lee, L. L.; Mullen, K. J. Random Walks in Nanotube Composites: Improved Algorithms and the Role of Thermal Boundary Resistance. *Appl. Phys. Lett.* **2005**, *87* (1), 013101.
(26) Einstein, A. The Electrodynamics of Moving Bodies. *Ann. Phys. (Amsterdam, Neth.)* **1905**, *17*, 891−921.
(27) Swartz, E. T.; Pohl, R. O. Thermal-Boundary Resistance. *Rev. Mod. Phys.* **1989**, *61* (3), 605−668.
(28) Balandin, A. A. Thermal properties of graphene and nanostructured carbon materials. *Nat. Mater.* **2011**, *10* (8), 569−581.
(29) Bui, K.; Papavassiliou, D. V. Numerical Calculation of the Effective Thermal Conductivity of Nanocomposites. *Numer. Heat Transfer, Part A* **2013**, *63* (8), 590−603.
(30) Duong, H. M.; Papavassiliou, D. V.; Mullen, K. J.; Wardle, B. L.; Maruyama, S. A Numerical Study on the Effective Thermal Conductivity of Biological Fluids Containing Single-Walled Carbon Nanotubes. *Int. J. Heat Mass Transfer* **2009**, *52* (23−24), 5591−5597.
(31) Duong, H. M.; Papavassiliou, D. V.; Mullen, K. J.; Maruyama, S. Computational Modeling of the Thermal Conductivity of Single-Walled Carbon Nanotube: Polymer Composites. *Nanotechnology* **2008**, *19* (6), 065702.
(32) Bui, K.; Grady, B. P.; Papavassiliou, D. V. Heat Transfer in High Volume Fraction CNT Nanocomposites: Effects of Inter-Nanotube Thermal Resistance. *Chem. Phys. Lett.* **2011**, *508* (4−6), 248−251.
(33) Fan, Z.; Gong, F.; Nguyen, S. T.; Duong, H. M. Advanced Multifunctional Graphene Aerogel: Poly (Methyl Methacrylate) Composites: Experiments and Modeling. *Carbon* **2015**, *81* (0), 396−404.
(34) Song, Y. S.; Youn, J. R. Influence of Dispersion States of Carbon Nanotubes on Physical Properties of Epoxy Nanocomposites. *Carbon* **2005**, *43* (7), 1378−1385.
(35) Cherkasova, A. S.; Shan, J. W. Particle Aspect-Ratio and Agglomeration-State Effects on the Effective Thermal Conductivity of Aqueous Suspensions of Multiwalled Carbon Nanotubes. *J. Heat Transfer* **2010**, *132* (8), 082402.
(36) Roy, A. K.; Farmer, B. L.; Varshney, V.; Sihn, S.; Lee, J.; Ganguli, S. Importance of Interfaces in Governing Thermal Transport in Composite Materials: Modeling and Experimental Perspectives. *ACS Appl. Mater. Interfaces* **2012**, *4* (2), 545−563.
(37) Jakubinek, M. B.; White, M. A.; Mu, M. F.; Winey, K. I. Temperature Dependence of Thermal Conductivity Enhancement in Single-Walled Carbon Nanotube/Polystyrene Composites. *Appl. Phys. Lett.* **2010**, *96* (8), 083105.
(38) Biercuk, M. J.; Llaguno, M. C.; Radosavljevic, M.; Hyun, J. K.; Johnson, A. T.; Fischer, J. E. Carbon Nanotube Composites for Thermal Management. *Appl. Phys. Lett.* **2002**, *80* (15), 2767−2769.
(39) Varshney, V.; Patnaik, S. S.; Roy, A. K.; Farmer, B. L. Modeling of Thermal Conductance at Transverse CNT−CNT Interfaces. *J. Phys. Chem. C* **2010**, *114* (39), 16223−16228.
(40) Gharib-Zahedi, M. R.; Tafazzoli, M.; Böhm, M. C.; Alaghemandi, M. Transversal Thermal Transport in Single-Walled Carbon Nanotube Bundles: Influence of Axial Stretching and Intertube Bonding. *J. Chem. Phys.* **2013**, *139* (18), 184704.
(41) Shenogin, S.; Bodapati, A.; Xue, L.; Ozisik, R.; Keblinski, P. Effect of Chemical Functionalization on Thermal Transport of Carbon Nanotube Composites. *Appl. Phys. Lett.* **2004**, *85* (12), 2229−2231.

DOI: 10.1021/acs.jpcc.5b00651
J. Phys. Chem. C XXXX, XXX, XXX−XXX